12/15-Lipoxygenase gene knockout severely impairs ischemia-induced angiogenesis due to lack of Rac1 farnesylation

Nikhlesh K. Singh,[1] Venkatesh Kundumani-Sridharan,[1] and Gadiparthi N. Rao[1]

[1]Department of Physiology, University of Tennessee Health Science Center, Memphis, TN

To understand the mechanisms by which 15(S)-hydroxyeicosatetraenoic acid (15(S)-HETE) activates Rac1 in the induction of angiogenesis, we studied the role of 3-hydroxy-3-methylglutaryl–coenzyme A (HMG-CoA) reductase and αPix. 15(S)-HETE stimulated Rac1 in a sustained manner in human dermal microvascular endothelial cells (HDMVECs). Simvastatin, a potent inhibitor of HMG-CoA reductase, suppressed 15(S)-HETE–induced Rac1 activation in HDMVECs affecting their migration and tube formation. 15(S)-HETE by inducing HMG-CoA reductase expression caused increased farnesylation and membrane translocation of Rac1 where it became activated by Src-dependent αPix stimulation. Mevalonate rescued 15(S)-HETE–induced Rac1 farnesylation and membrane translocation in HDMVECs and the migration and tube formation of these cells from inhibition by simvastatin. Down-regulation of αPix inhibited 15(S)-HETE–induced HDMVEC migration and tube formation. Hind-limb ischemia induced Rac1 farnesylation and activation leading to increased angiogenesis and these effects were blocked by simvastatin and rescued by mevalonate in WT mice. In contrast, hind-limb ischemia failed to induce Rac1 farnesylation and activation as well as angiogenic response in 12/15-Lox$^{-/-}$ mice. Activation of Src and αPix were also compromised at least to some extent in 12/15-Lox$^{-/-}$ mice compared with WT mice in response to hind-limb ischemia. Together, these findings demonstrate for the first time that HMG-CoA reductase plays a determinant role in 12/15-Lox–induced angiogenesis. (*Blood*. 2011;118(20):5701-5712)

Introduction

Besides its role in development, angiogenesis influences various disease processes. A large body of data indicates that angiogenesis plays a role in ocular and vascular diseases as well as tumor growth.[1] Paradoxically, in some diseases such as coronary artery disease angiogenesis plays a therapeutic role.[2] A broad range of molecules including growth factors, interleukins, and lipid molecules have been shown to modulate angiogenesis.[3-8] It was shown that interplay between these various angiogenic factors/molecules is required for the orchestrated process of angiogenesis.[9] In the past several years, work from various laboratories including ours had revealed that eicosanoids, the oxygenated metabolites of arachidonic acid (AA) influence angiogenesis.[10-17] Reinforcement of a role for eicosanoids in the regulation of angiogenesis can also be drawn by the demonstrations that while ω-6 polyunsaturated fatty acids (ω-6 PUFA) promote angiogenesis, ω-3 PUFA suppresses these effects.[18,19] In this aspect, it was shown that cytosolic phospholipase A_2 ($cPLA_2$) that liberates AA from the sn-2 position of glycerophospholipids, exerts a positive effect on the regulation of angiogenesis.[20] Furthermore, numerous studies have shown that cyclooxygenase, lipoxygenase and cytochrome P450 monooxygenase, the 3 pathways by which AA converts into various eicosanoids, are linked to regulation of both embryonic and pathologic angiogenesis.[10-17,21,22]

In gaining more insight into the mechanisms of eicosanoid-induced angiogenesis, we have shown that 15(S)-hydroxyeicosatetraenoic acid (15(S)-HETE), the major product of AA metabolism via the 15-Lox, possesses the capacity to stimulate various signaling molecules, including Src, phosphatidylinositol 3-kinase (PI3K), Akt, MAP kinase/ERK kinase 1 (MEK1), and c-Jun N-terminal kinase 1 (JNK1) leading to activation of transcriptional factors such as activating transcriptional factor 2 (ATF2), activator protein 1 (AP1), early growth response factor 1 (Egr1), and signal transducers and activators of transcription (STATs) and thereby influencing the expression of angiogenic molecules such as fibroblast growth factor 2 (FGF2), vascular endothelial growth factor (VEGF) and IL-8 and promoting autocrine-mediated angiogenesis [11-15, 17, 23-25]. Among the signaling molecules that are robustly and sustainably activated by 15(S)-HETE in microvascular endothelial cells of various vascular beds are Src, a non-receptor tyrosine kinase[24] and Rac1, a Rho GTPase.[23] Both Src and Rac1 play important roles in the regulation of cell proliferation and migration.[26-30] Previously, we have reported that 15(S)-HETE–induced migration and tube formation of human retinal microvascular endothelial cells (HRMVECs) require Src-mediated Rac1 activation.[23] To understand the mechanisms of sustained activation of Rac1 by 15(S)-HETE in enhancing endothelial cell (EC) migration and tube formation, we have studied the role of its farnesylation as well as GDP/GTP exchangers. In the present work, we demonstrate that 12/15-Lox–15(S)-HETE via inducing the expression of HMG-CoA reductase facilitates the farnesylation and translocation of Rac1 to plasma membrane, where it becomes activated by Src-dependent αPix-mediated GDP/GTP exchange in human dermal microvascular endothelial cells (HDMVECs). In addition, our results show that HMG-CoA reductase-dependent farnesylation and αPix-dependent GDP/GTP exchange of Rac1 is essential for 12/15-Lox–15(S)-HETE–induced angiogenesis in response to hind-limb ischemia.

Methods

Reagents

15(S)-HETE was bought from Cayman Chemicals. Growth factor–reduced Matrigel was obtained from BD Biosciences. Anti-pSrc (Y416) antibodies

Submitted April 7, 2011; accepted August 8, 2011. Prepublished online as *Blood* First Edition paper, August 12, 2011; DOI 10.1182/blood-2011-04-347468.

The publication costs of this article were defrayed in part by page charge payment. Therefore, and solely to indicate this fact, this article is hereby marked "advertisement" in accordance with 18 USC section 1734.

An Inside *Blood* analysis of this article appears at the front of this issue.

were bought from Cell Signaling Technology. Anti-HMGCoA reductase, anti-PY20, anti-Rac1 and anti-Src antibodies were obtained from Millipore. Anti–β-tubulin (SC-9104) and anti-αPix (SC-10 927) antibodies were purchased from Santa Cruz Biotechnology. Anti-CD31 antibodies were obtained from BD Pharmingen. Anti-von Willebrand Factor (vWF) antibodies were supplied by Abcam. Hoechst 33 342 (H3570), Lipofectamine 2000 reagent and Prolong Gold antifade mounting medium (P36930) were bought from Invitrogen. Simvastatin was purchased from Enzo Lifesciences. Actinomycin D, cycloheximide and mevalonolactone were bought from Sigma Aldrich. Human αPix siRNA and siCONTROL non-targeting siRNA were bought from Dharmacon RNAi Technologies. The Animal Care and Use Committee of the University of Tennessee Health Science Center approved all the protocols involving the use of animals.

Adenoviral vectors

The construction of Ad-GFP and Ad-dnSrc were described previously.[23,31]

Cell culture

HDMVECs were bought from Cascade Biologics. HDMVECs were grown in medium 131 containing microvascular growth supplements (MVGSs), 10 μg/mL gentamycin, and 0.25 μg/mL amphotericin B. Cultures were maintained at 37°C in a humidified 95% air and 5% CO_2 atmosphere. HDMVECs were growth-arrested by incubating in medium 131 for 24 hours and used to perform the experiments unless otherwise indicated.

Transfections and transductions

HDMVECs were transfected with control or test siRNA molecules at a final concentration of 100nM using Lipofectamine 2000 transfection reagent according to the manufacturer's instructions. In the case of adenoviral vectors, cells were transduced with the adenovirus carrying GFP or target molecule at 40 moi overnight in complete medium. After transfections or transductions, cells were growth-arrested for 24 hours and used as required. To deliver siRNA molecules in vivo, 3 μg of siRNA was mixed with 200 μL of 30% pluronic gel and it was applied around the ligated femoral artery immediately after the surgery.

Cell migration

Cell migration was performed using a modified Boyden chamber method as described previously.[25] Vehicle or 15(S)-HETE were added to the lower chamber at the indicated concentrations. Both the upper and lower chambers contained medium 131. When the effect of a specific siRNA was tested on 15(S)-HETE–induced HDMVEC migration, cells were transfected with scrambled or test siRNA and growth-arrested before they were subjected to migration assay. In the case of testing the effects of pharmacologic agents, cells were treated first with the agent for 30 minutes at 37°C and then subjected to migration assay. After 6 hours of incubation at 37°C, non-migrated cells were removed from the upper side of the membrane with cotton swabs, and the cells on the lower surface of the membrane were fixed in methanol for 15 minutes. The membrane was then stained with DAPI in VECTASHIELD mounting medium (Vector Laboratories) and observed under Nikon Diaphot fluorescence microscope with photometrics CH250 CCD camera (Nikon). Cells were counted in 6 randomly selected squares per well and presented as number of migrated cells per field.

Tube formation

Tube formation assay was performed using 24-well plates coated with growth factor-reduced Matrigel as described previously.[25] The treatment conditions were the same as those applied in migration assay. Vehicle or 15(S)-HETE, at the indicated concentrations, were added to the appropriate well and the cells were incubated at 37°C for 6 hours. When the effects of a specific siRNA or pharmacologic agent were tested on 15(S)-HETE–induced HDMVEC tube formation, cells were subjected to this regimen exactly as described in cell migration followed by tube formation assay. Tube formation was observed under an inverted microscope (Eclipse TS100; Nikon). Images were captured with a CCD color camera (KP-D20AU; Hitachi) attached to the microscope and tube length was measured using the National Institutes of Health (NIH) ImageJ 1.421 software.

Membrane and cytoplasmic fractions

After appropriate treatments, HDMVECs were washed twice with ice-cold PBS containing 10mM NaF, 10mM β-glycerophosphate, 2 mg/mL leupeptin, 10 mg/mL aprotinin, and 1mM PMSF. Cells were scraped, dispersed by Teflon-glass Dounce homogenizer with 50 strokes on ice and lysed by sonication at half maximal speed for 15 seconds with 10 seconds interval for a total of 4 minutes. The resulting cell extracts were centrifuged at 3000*g* for 10 minutes to remove the cell debris. The resulting supernatant was subjected to centrifugation at 30 000*g* for 30 minutes at 4°C and the membrane (pellet) and cytoplasmic (supernatant) fractions were collected. The membrane pellet was dissolved in 10mM Tris-HCl buffer (pH 7.4) containing 0.3% SDS, 2 mg/mL leupeptin, 10 mg/mL aprotinin, and 1mM PMSF. After determining protein concentrations using BCA reagent, both the membrane and cytoplasmic fractions were analyzed by Western blotting using specific antibodies.

Western blotting

After appropriate treatments and rinsing with cold PBS, HDMVECs were lysed in 500 μL lysis buffer (PBS, 1% nonidet P-40, 0.5% sodium deoxycholate, 0.1% SDS, 100 μg/mL PMSF, 100 μg/mL aprotinin, 1 μg/mL leupeptin, and 1mM sodium orthovanadate) and scraped into 1.5 mL Eppendorf tubes. After standing on ice for 20 minutes, the cell lysates were cleared by centrifugation at 12 000 rpm for 20 minutes at 4°C. Cell lysates containing an equal amount of protein were resolved by electrophoresis on 0.1% SDS and 10% polyacrylamide gels. The proteins were transferred electrophoretically to a nitrocellulose membrane. After blocking in 10mM Tris-HCl buffer, pH 8.0, containing 150mM sodium chloride, 0.1% Tween 20 and 5% (wt/vol) non-fat dry milk, the membrane was treated with appropriate primary antibodies followed by incubation with HRP-conjugated secondary antibodies. The antigen-antibody complexes were detected using chemiluminescence reagent kit (GE Healthcare).

Pull-down assay

An equal amount of protein from control and each treatment was incubated with GST-PAK1 (Cdc42 and Rac1 interactive binding domain)–conjugated Sepharose CL4B beads for 45 minutes at 4°C. The beads were collected by centrifugation, washed in lysis buffer, heated in Laemmeli sample buffer for 5 minutes and the released proteins were resolved on 0.1% SDS-12% PAGE and immunoblotted with anti-Rac1 antibodies. After incubation with HRP-conjugated secondary antibodies, the antigen-antibody complexes were detected using a chemiluminescence reagent kit.

Real-time reverse RT-PCR

After appropriate treatments, total cellular RNA was isolated from HDMVECs using RiboPure Kit as per the manufacture's instructions (Ambion). Reverse transcription was carried out with High Capacity cDNA reverse transcription kit for RT-PCR based on supplier's protocol (Applied Biosystems). The cDNA was then used as template for PCR using TaqMan Gene Expression Assays for human HMG-CoA reductase and human β-actin (Hs01102991_g1 and Hs99999903_m1, respectively) and murine HMG-CoA reductase and murine β-actin (Mm01282499_m1 and Mm02619580_g1, respectively) were purchased from Applied Biosystems. The amplification was carried out on Applied Biosystems 7300 real-time PCR Systems (Applied Biosystems) using the following conditions: 95°C for 10 minutes followed by 40 cycles at 95°C for 15 seconds with final extension at 60°C for 1 minute for both HMG-CoA reductase and β-actin. The PCR-amplification was examined using the 7300 real-time PCR system operated SDS Version 1.4 program. The program uses the Delta Rn analysis method (Applied Biosystems).

Hind-limb ischemia

Hind-limb ischemia was induced in wild-type mice as previously reported by ligating the left common femoral artery proximal to origin of the profunda femoris artery.[25] Mice were anesthetized with intraperitoneal injection of ketamine (100 mg/kg) and xylazine (8 mg/kg). Aseptic surgery was performed to ligate the left common femoral artery as follows. An incision was made in left groin of mice. Blunt dissection was performed and the left common femoral artery was identified by its pale pink color and pulsatile nature. The common femoral vein and femoral nerve were dissected free of the artery. Two ligations were performed in the common femoral artery proximal to the origin of the profunda femoris artery using 6.0 nylon sutures. The common femoral artery was then transected between the ligation sites. Immediate blanching was noted in the distal left hind limb after ligation. The incision was sutured in a single layer using the same suture material as for ligation. Two days before surgery, intraperitoneal injections of simvastatin (5 mg/kg body weight) and mevalonate (10 mg/kg body weight) were given to mice everyday until the completion of the experiment. Mice were noted to be limping and dragging the left hind limb after recovery from anesthesia.

Double immunofluorescence staining

After dissecting out adductor muscles from mice, they were snap-frozen in OCT compound. Cryosections (5 μm) were made using Leica Kryostat (Model: CM3050S, Leica). After blocking in normal goat serum, the cryosections were incubated with rabbit anti–mouse von Willebrand Factor (vWF) antibodies and rat anti–mouse CD31 antibodies or anti–HMG-CoA reductase antibodies for 1 hour. After washing in PBS, all slides were incubated with goat anti–rabbit secondary antibodies conjugated with Alexa Fluor 568 or goat anti–rat secondary antibodies conjugated with Alexa Fluor 488 or goat anti–rat secondary antibodies conjugated with Alexa Fluor 568. To study translocation of Rac1, HDMVECs were grown on cell culture grade coverslips to 40% confluence, quiesced and treated with vehicle or 0.1μM 15(S)-HETE for 30 minutes in combination with or without 10μM simvastatin and/or 50μM mevalonate. After treatment, cells were washed with PBS and fixed with 3% paraformaldehyde for 10 minutes at 37°C. To retrieve antigen, cells were treated at 65°C for 20 minutes in sodium citrate buffer (10mM sodium citrate, 0.05% Tween 20, pH 6.0), blocked and permeabilized in PBS containing 3% BSA and 0.5% Triton X-100 for 15 minutes at room temperature. Permeabilized cells were incubated first with anti-Rac1 antibodies (1:200 dilution in PBS) followed by goat anti–mouse secondary antibodies conjugated with Alexa Fluor 568, counterstained with HOECHST 33 342 (1:3000 dilution in PBS) for 1 minute at room temperature and mounted onto glass slides with Prolong Gold antifade mounting medium. Fluorescence images of cells were captured using an inverted Zeiss fluorescence microscope (AxioVision AX10) via a 40× NA 0.6 objective and AxioCam MRm camera without any enhancements.

Statistics

All the experiments were repeated 3 times and data are presented as means ± SD. The treatment effects were analyzed by Student *t* test, and the *P* values $< .05$ were considered statistically significant. In the case of double immunofluorescence staining and Western blotting, 1 representative set of data are shown.

Results

Simvastatin inhibits 15(S)-HETE–induced Rac1 farnesylation and activation

Previously we have reported that 15(S)-HETE activates Rac1 in both HDMVECs and HRMVECs facilitating their migration and tube formation.[23,25] To understand the mechanisms by which 15(S)-HETE activates Rac1 in these cells, we have studied the role of HMG-CoA reductase and RhoGEFs as these molecules play an important role in RhoGTPase farnesylation and GDP/GTP exchange, respectively.[32-35] In agreement with our previous observations, 15(S)-HETE (0.1μM) stimulated Rac1 in a time-dependent manner (Figure 1A). Simvastatin, a potent inhibitor of HMG-CoA reductase, blocked 15(S)-HETE–induced Rac1 activation (Figure 1B). Consistent with its effect on Rac1 activation, simvastatin also inhibited 15(S)-HETE–induced HDMVEC migration and tube formation (Figure 1C-D). Because the role of HMG-CoA reductase in the regulation of RhoGTPases lies at the level of their farnesylation, next we wanted to find whether Rac1 gets farnesylated in response to 15(S)-HETE. 15(S)-HETE–induced Rac1 farnesylation in a time-dependent manner (Figure 2A). In addition, simvastatin reduced 15(S)-HETE–induced Rac1 farnesylation (Figure 2B). If simvastatin blockade of Rac1 activation was because of its inhibition of HMG-CoA reductase activity affecting the production of isoprenoids then one would expect that exogenous addition of HMG-CoA reductase product, and isoprenoid precursor, mevalonate should overcome the inhibitory effect of simvastatin on 15(S)-HETE–induced Rac1 farnesylation and activation. Indeed, exogenous addition of mevalonate rescued 15(S)-HETE–induced Rac1 farnesylation and activation from inhibition by simvastatin (Figure 2B). Because farnesylation of Rac1 is required for its membrane translocation, we asked the question whether inhibition of HMG-CoA reductase by simvastatin prevents Rac1 translocation from the cytoplasm to the membrane and mevalonate rescues these effects. Treatment of cells with 15(S)-HETE led to increased translocation of Rac1 from the cytoplasm to the membrane and this response was substantially blocked by simvastatin (Figure 2B-C). Furthermore, simultaneous addition of mevalonate rescued 15(S)-HETE–induced membrane translocation of Rac1 from inhibition by simvastatin (Figure 2B-C). Consistent with these observations, mevalonate also rescued 15(S)-HETE–induced HDMVEC migration and tube formation from inhibition by simvastatin (Figure 2D-E). Mevalonate alone had no effect on Rac1 farnesylation and its membrane translocation and activation (Figure 2B-C). In line with these observations, mevalonate alone also had no effect on HDMVEC migration and tube formation (Figure 2D-E).

15(S)-HETE induces HMG-CoA reductase expression in HDMVECs

To find the mechanism by which 15(S)-HETE stimulates Rac1 farnesylation, we have studied its effect on the expression of HMG-CoA reductase. 15(S)-HETE–induced HMG-CoA reductase mRNA levels in a time-dependent manner with a 2-fold increase at 1 hour and this effect was sustained till 2 hours (Figure 3A). To confirm this result, we also tested the effect of 15(S)-HETE on HMG-CoA reductase protein levels. Consistent with its effect on HMG-CoA reductase mRNA levels, 15(S)-HETE–induced HMG-CoA reductase expression at protein level as well (Figure 3B). Because 15(S)-HETE–induced HMG-CoA reductase expression very rapidly, we asked the question whether this effect is at transcriptional level and requires new protein synthesis. To obtain clues into these possibilities, we tested the effects of actinomycin-D (Act-D) and cycloheximide (CHM), RNA polymerase II and protein synthesis inhibitors, respectively, on 15(S)-HETE–induced HMG-CoA reductase mRNA and protein levels. Both the inhibitors blocked HMG-CoA reductase expression almost completely at mRNA and protein levels (Figure 3C-D). These results infer that 15(S)-HETE induces HMG-CoA reductase expression at transcriptional level and requires new protein synthesis. To find whether induction of expression of HMG-CoA reductase at transcriptional

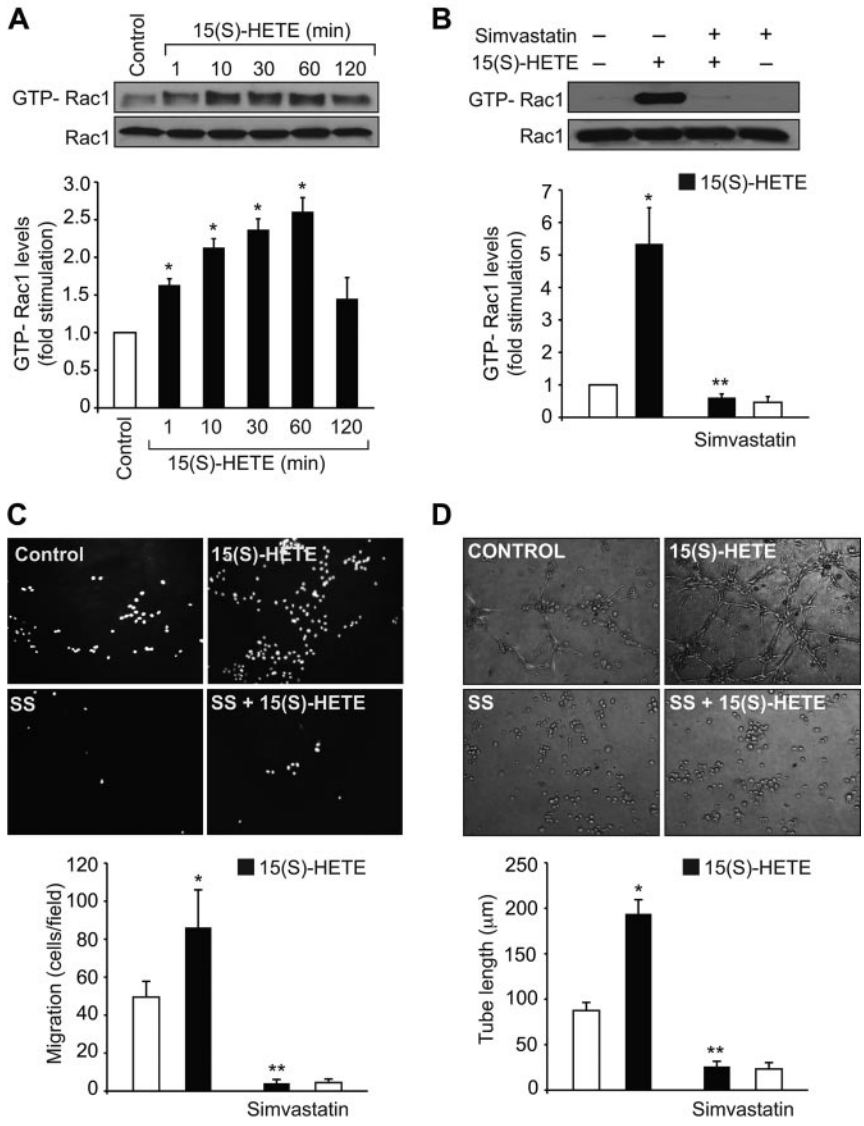

Figure 1. Simvastatin inhibits 15(S)-HETE–induced Rac1 activation in HDMVECs and suppresses their migration and tube formation. (A,B) Quiescent HDMVECs were treated with and without 0.1μM 15(S)-HETE for the indicated time periods or 60 minutes in the presence and absence of 10μM simvastatin and Rac1 activation was measured by pull-down assay. Total cellular Rac1 levels were measured by Western blotting. (C,D) Quiescent HDMVECs that were treated with and without simvastatin were subjected to 15(S)-HETE–induced migration (C) or tube formation (D). The bar graphs represent the mean ± SD values of 3 independent experiments. $*P < .01$ versus control, $**P < .01$ versus 15(S)-HETE.

level is required for Rac1 farnesylation, we tested the effect of Act-D. Act-D completely blocked 15(S)-HETE–induced Rac1 farnesylation (Figure 3E).

15(S)-HETE–induced Rac1 activation requires Src-dependent αPix stimulation

To find the RhoGEFs that mediate 15(S)-HETE–induced Rac1 activation, we have examined the role of αPix. 15(S)-HETE stimulated the tyrosine phosphorylation of αPix in a time-dependent manner (Figure 4A). Because our previous studies showed that 15(S)-HETE stimulates Src,[24,25] we asked the question whether this non-receptor tyrosine kinase plays a role in 15(S)-HETE–induced αPix phosphorylation. Adenovirus-mediated transduction of dominant negative Src completely blocked 15(S)-HETE–induced αPix phosphorylation (Figure 4B). To test the effect of αPix on 15(S)-HETE–induced Rac1 activation, we used siRNA approach. As shown in Figure 4C, αPix siRNA but not scrambled RNA depleted αPix steady-state levels by ~65%. Down-regulation of αPix levels by its siRNA also inhibited 15(S)-HETE–induced Rac1 activation (Figure 4D). Similarly, siRNA-mediated down-regulation of αPix levels blocked 15(S)-HETE–induced HDMVEC migration and tube formation substantially (Figure 4E-F).

Lack of angiogenic response to hind-limb ischemia in 12/15-Lox$^{-/-}$ mice

12/15-Lox is the murine ortholog of human 15-Lox1. Therefore, to extend the in vitro observations to in vivo, we used 12/15-Lox$^{-/-}$ mice. Hind-limb ischemia induced angiogenesis in WT mice as measured by blood perfusion using Laser Doppler Perfusion Imager. However, hind-limb ischemia failed to trigger a similar angiogenic response in 12/15-Lox$^{-/-}$ mice (Figure 5A). To confirm these observations, we have isolated adductor muscles from WT and 12/15-Lox$^{-/-}$ mice, made sections and immunostained for CD31 and vWF. Double immunofluorescence staining of adductor muscle sections for CD31 and vWF revealed that hind-limb ischemia increases the number of new blood vessels in the adductor muscles of WT mice compared with 12/15-Lox$^{-/-}$ mice (Figure 5B). Because 15(S)-HETE activates Rac1 very robustly, we next asked the question whether the lack of angiogenic response to hind-limb ischemia in 12/15-Lox$^{-/-}$ mice was because of lack of

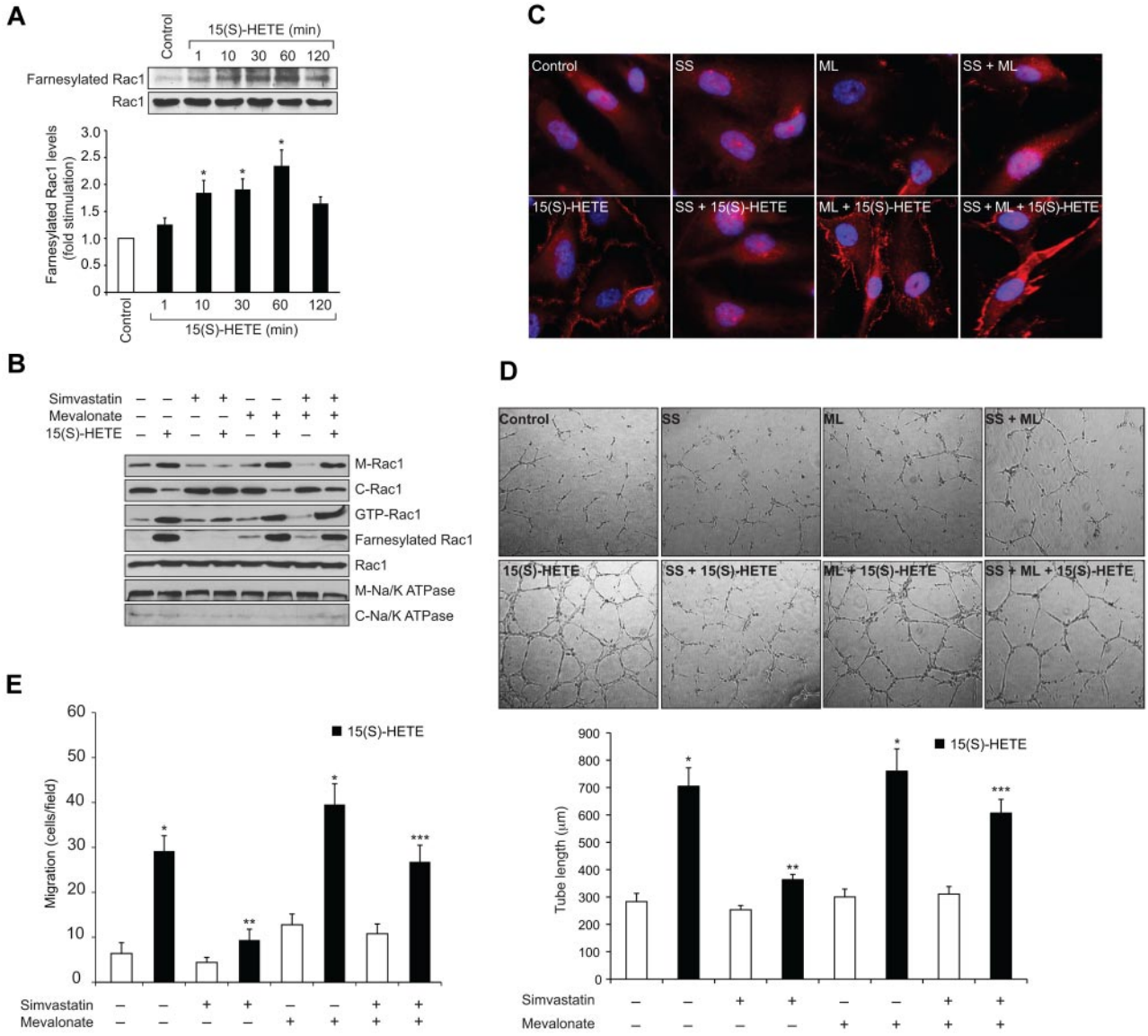

Figure 2. Mevalonate rescues 15(S)-HETE–induced farnesylation, membrane translocation and activation of Rac1 in HDMVECs and the migration and tube formation of these cells from inhibition by simvastatin. (A-B) Quiescent HDMVECs were treated with and without 0.1μM 15(S)-HETE for the indicated time periods or 60 minutes in the presence and absence of 10μM simvastatin in combination with or without 50μM mevalonate and either whole cellular extracts or the cytoplasmic and membrane fractions were prepared. Rac1 farnesylation was measured by immunoprecipitation of an equal amount of protein with anti-farnesyl antibodies followed by immunoblotting with anti-Rac1 antibodies. Rac1 activation was measured by pull-down assay. Rac1 and Na/K ATPase levels were measured by Western blotting using their specific antibodies. (C) All the conditions were the same as in panel B, except that cells were fixed, permeabilized and immunostained for Rac1 using anti-Rac1 antibodies followed by probing with Alexa Fluor 568–conjugated secondary antibodies. (D-E) HDMVECs were treated with or without 10μM simvastatin in the presence and absence of 50μM mevalonate, trypsinized, rinsed with TNS and subjected to 15(S)-HETE (0.1μM)–induced tube formation (D) or migration (E). The bar graphs in panels A, D and E represent the mean ± SD values of 3 independent experiments. *$P < .01$ versus control; **$P < .01$ versus 15(S)-HETE; ***$P < .01$ versus simvastatin + 15(S)-HETE. C indicates cytoplasmic fraction; M, membrane fraction; ss, simvastatin; and ML, mevalonate.

activation of Rac1. To address this postulation, 7 days after ligation of femoral artery, tissue extracts of adductor muscles from both WT and 12/15-Lox$^{-/-}$ mice were prepared and analyzed for GTP-bound Rac1. Hind-limb ischemia induced Rac1 activation by ~ 3-fold compared with control in WT mice (Figure 5C). In contrast, hind-limb ischemia had no such effect on Rac1 activation in 12/15-Lox$^{-/-}$ mice. To understand the mechanism(s) for the lack of a response in the activation of Rac1 in 12/15-Lox$^{-/-}$ mice compared with WT mice in response to hind-limb ischemia, we have measured Rac1 farnesylation. Interestingly, hind-limb ischemia increased farnesylation of Rac1 only in WT mice but not in 12/15-Lox$^{-/-}$ mice (Figure 5C). To test whether the lack of Rac1 farnesylation in 12/15-Lox$^{-/-}$ mice was because of alterations in the expression levels of HMG-CoA reductase, we studied the effect of hind-limb ischemia on its mRNA and protein levels. Hind-limb ischemia induced HMG-CoA reductase expression at both mRNA and protein levels only in WT mice but not in 12/15-Lox$^{-/-}$ mice (Figure 5D-E). To find whether the increased expression of HMG-CoA reductase occurs in ECs, we have performed double immunofluorescence staining of adductor muscle sections for HMG-CoA reductase and CD31. As shown in Figure 5F, hind-limb ischemia increased the expression of HMG-CoA reductase mainly in ECs. To validate the role of HMG-CoA reductase in hind-limb ischemia-induced Rac1 activation and angiogenesis further, we used a pharmacological approach. Intraperitoneal injection of simvastatin (5 mg/kg/d/9 days) blocked hind-limb ischemia-induced Rac1

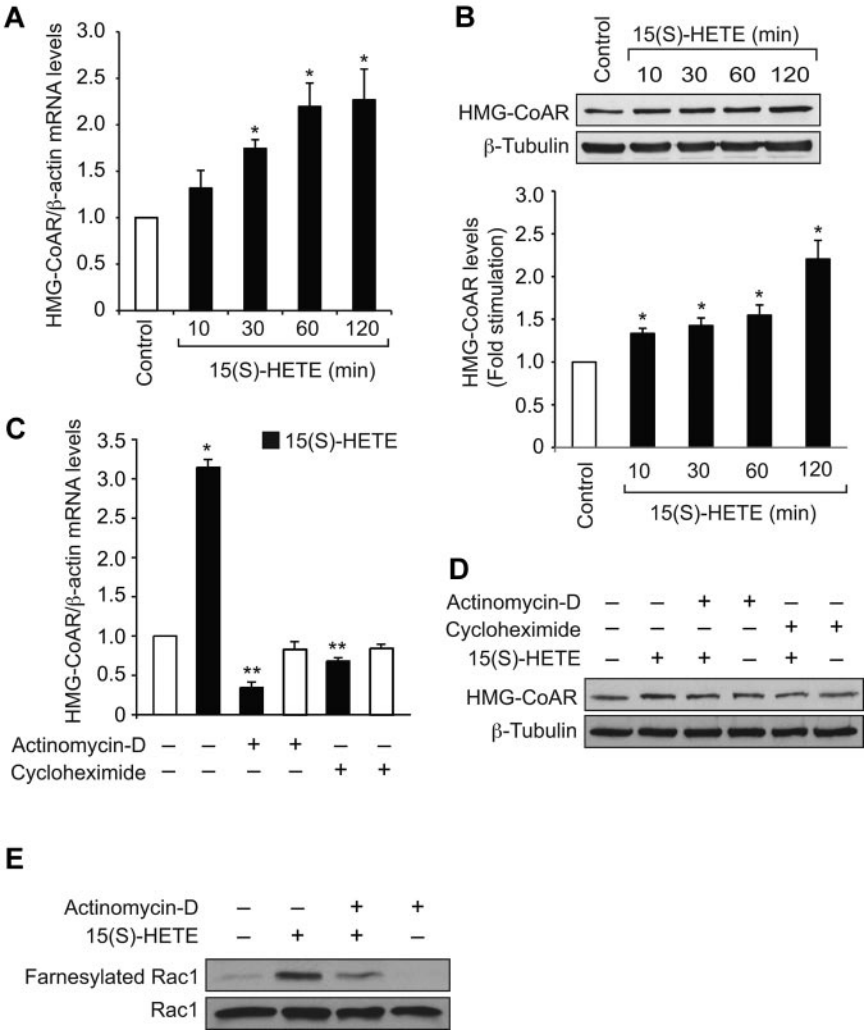

Figure 3. 15(S)-HETE induces HMG-CoA reductase expression in HDMVECs. (A-B) Quiescent HDMVECs were treated with and without 0.1 μM 15(S)-HETE for the indicated time periods and either total cellular RNA was isolated or cell extracts were prepared. The RNA was analyzed for HMG-CoA reductase mRNA levels by QRT-PCR (A) and the cell extracts were analyzed for HMG-CoA reductase protein levels by Western blotting (B). (C-D) Quiescent HDMVECs were treated with 0.1 μM 15(S)-HETE in the presence or absence of 20 μg/mL actinomycin D or 10 μg/mL cycloheximide for 2 hours and HMG-CoA reductase mRNA and protein levels were measured as described in panels A and B, respectively. (E) Quiescent HDMVECs that were pretreated with actinomycin D (20 μg/mL) for 2 hours were treated with and without 15(S)-HETE (0.1 μM) for 10 minutes and cell extracts were prepared. An equal amount of protein from control and each treatment was immunoprecipitated with anti-Farnesyl antibodies and immunocomplexes were analyzed by Western blotting for Rac1 using anti-Rac1 antibodies. Total cellular Rac1 levels were measured by Western blotting. The bar graphs in panels A, B and C represent the mean ± SD values of 3 independent experiments. *$P < .01$ versus control; **$P < .01$ versus 15(S)-HETE. HMG-CoAR indicates HMG-CoA reductase.

farnesylation and activation in WT mice (Figure 6A). Simvastatin also suppressed hind-limb ischemia-induced angiogenesis (Figure 6B-C). In addition, simultaneous administration of mevalonate along with simvastatin (10 mg/kg/d/9 days) rescued hind-limb ischemia-induced Rac1 farnesylation and activation resulting in the recovery of angiogenic response from inhibition by simvastatin (Figure 6A-C). Mevalonate alone, however, had no additional effect on Rac1 farnesylation/activation and angiogenesis than what was observed with ischemia (Figure 6A-C). If the lack of angiogenic response to hind-limb ischemia in 12/15-Lox$^{-/-}$ mice was because of a reduction in HMG-CoA reductase induction levels, then one would expect that supplementing these mice with mevalonate should alleviate this defect. Administration of 12/15-Lox$^{-/-}$ mice with mevalonate restored the ability of these mice to respond to hind-limb ischemia in the stimulation of Rac1 farnesylation and activation as well as angiogenesis only partially (Figure 7A-B). In regard to Src and αPix, hind-limb ischemia increased tyrosine phosphorylation of both these molecules in WT and 12/15-Lox$^{-/-}$ mice, although the response was much lower in the latter group of mice compared with the former group (Figure 8A). Furthermore, down regulation of αPix levels by its siRNA attenuated hind-limb ischemia-induced Rac1 activation and angiogenesis in WT mice (Figure 8B-C).

Discussion

The important observations of the present study are as follows: (1) 15(S)-HETE stimulated Rac1 farnesylation and activation very robustly and sustainably in HDMVECs; (2) simvastatin inhibited 15(S)-HETE–induced Rac1 farnesylation and activation resulting in reduced migration and tube formation of HDMVECs and exogenous addition of mevalonate rescued these effects; (3) 15(S)-HETE induced the expression of HMG-CoA reductase in a time-dependent manner at both mRNA and protein levels; (4) 15(S)-HETE–induced Rac1 activation exhibited a requirement for Src-mediated αPix activation; (5) down-regulation of αPix levels blocked 15(S)-HETE–induced Rac1 activation in HDMVECs and the migration and tube formation of these cells; (6) hind-limb ischemia-induced angiogenesis was found to be significantly higher in WT mice compared with 12/15-Lox$^{-/-}$ mice; (7) hind-limb ischemia also induced Rac1 farnesylation and activation more robustly in WT mice compared with 12/15-Lox$^{-/-}$ mice; (8) hind-limb ischemia induced the expression of HMG-CoA reductase in ECs of adductor muscles of WT mice only but not in 12/15-Lox$^{-/-}$ mice; (9) simvastatin inhibited hind-limb ischemia-induced Rac1 farnesylation and activation leading to a reduction of

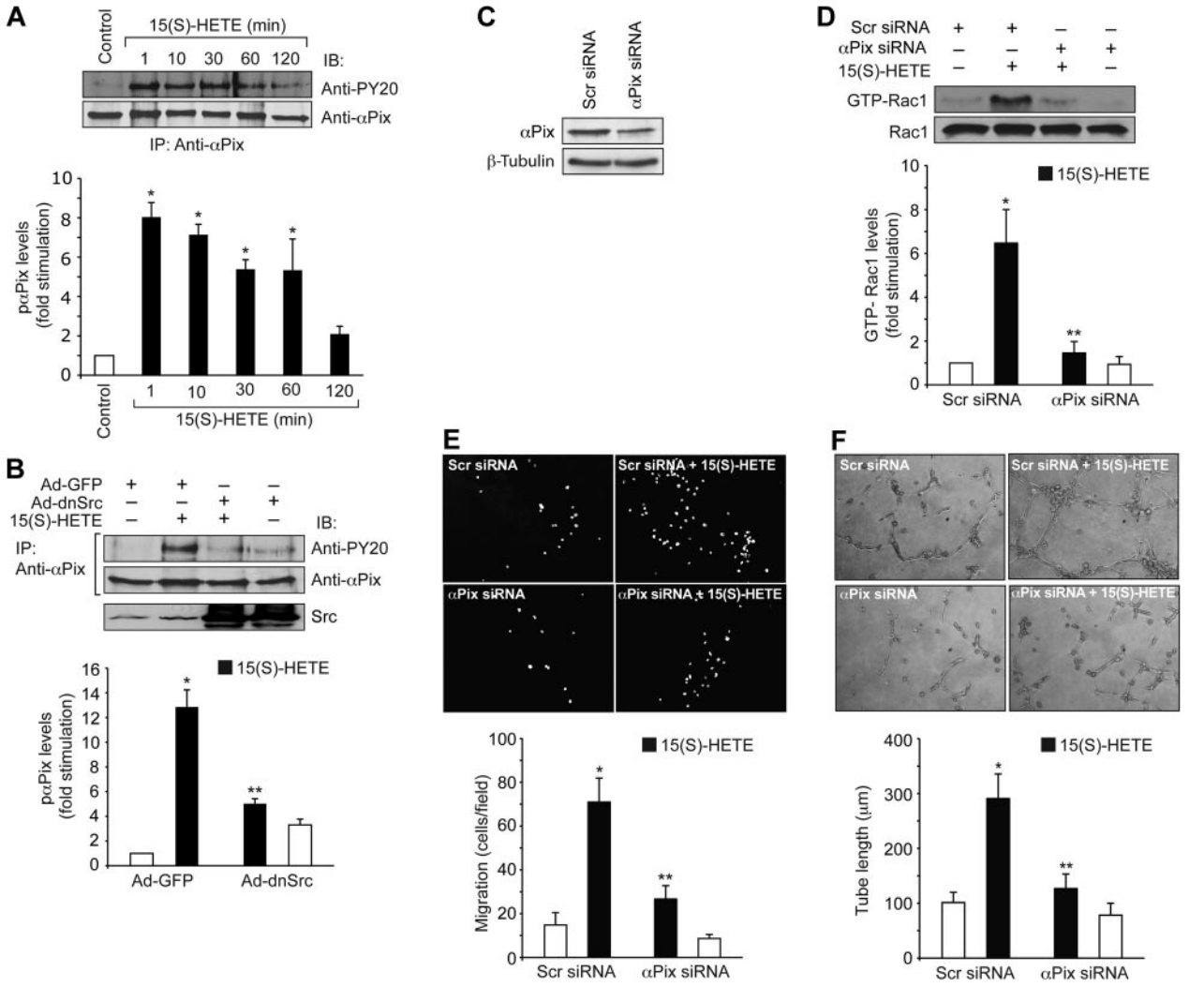

Figure 4. 15(S)-HETE induces αPix tyrosine phosphorylation in Src-dependent manner. (A) Quiescent HDMVECs were treated with and without 0.1μM 15(S)-HETE for the indicated time periods and αPix tyrosine phosphorylation was measured by immunoprecipitation with anti-αPix antibodies followed by immunoblotting with anti-PY20 antibodies. (B) Cells were transduced with Ad-GFP or Ad-dnSrc, growth-arrested, treated with and without 0.1μM 15(S)-HETE for 10 minutes and analyzed for αPix tyrosine phosphorylation as described in panel A. (C) HDMVECs were transfected with scrambled (Scr) or αPix siRNA and 48 hours later cell extracts were prepared and analyzed for αPix levels by Western blotting using its specific antibodies. (D) HDMVECs that were transfected with scrambled or αPix siRNA and growth-arrested were treated with and without 0.1μM 15(S)-HETE for 1 hour and Rac1 activation was measured. (E-F) All the conditions were the same as in panel D except that cells were subjected to 0.1μM 15(S)-HETE-induced migration (E) or tube formation (F). The bar graphs represent the mean ± SD values of 3 independent experiments. *$P < .01$ versus control; **$P < .01$ versus 15(S)-HETE.

angiogenesis in WT mice and administration of mevalonate rescued these effects; (10) supplementation of mevalonate restored the ability of 12/15-Lox$^{-/-}$ mice to farnesylate and activate Rac1 as well as to induce angiogenesis in response to ischemia modestly; (11) hind-limb ischemia activated both Src and αPix in WT as well as 12/15-Lox$^{-/-}$ mice, although the response in the latter group of mice was much lower compared with the former group; and (12) down-regulation of αPix levels attenuated ischemia-induced Rac1 activation and angiogenesis. Together, these observations suggest that 12/15-Lox-12/15(S)-HETE–induced angiogenesis requires HMG-CoA reductase-dependent farnesylation and Src-dependent αPix-mediated activation of Rac1.

Rac1 via its involvement in the modulation of cytoskeletal remodeling plays an important role in cell migration and proliferation.[28-30] We have previously reported that 15(S)-HETE induces HDMVEC migration and tube formation.[25] Both these events require cytoskeletal remodeling. In this aspect, 15(S)-HETE stimulated Rac1 very robustly, which in turn, correlated with migration and tube formation of HDMVECs. In the present study, we observed that 15(S)-HETE induces HMG-CoA reductase expression in HDMVECs. HMG-CoA reductase is a rate-limiting enzyme in the biosynthesis of cholesterol.[36] In addition to its role in cholesterol biosynthesis, via producing isoprenoids and thereby promoting isoprenylation, HMG-CoA reductase facilitates membrane targeting of proteins such as Rho GTPases.[37] It appears that 15(S)-HETE via inducing the expression of HMG-CoA reductase stimulates the isoprenylation of Rac1 and its translocation to plasma membrane. In fact, inhibition of HMG-CoA reductase results in the suppression of 15(S)-HETE–induced Rac1 farnesylation, its membrane translocation and activation, suggesting that HMG-CoA reductase via modulating Rac1 farnesylation plays an important role in 15(S)-HETE–induced angiogenic responses in HDMVECs. The inhibition of HMG-CoA reductase expression by Act-D led to a decrease in 15(S)-HETE–induced Rac1 farnesylation, a finding that also supports a role for HMG-CoA reductase in 15(S)-HETE–induced Rac1 activation and angiogenesis. The role

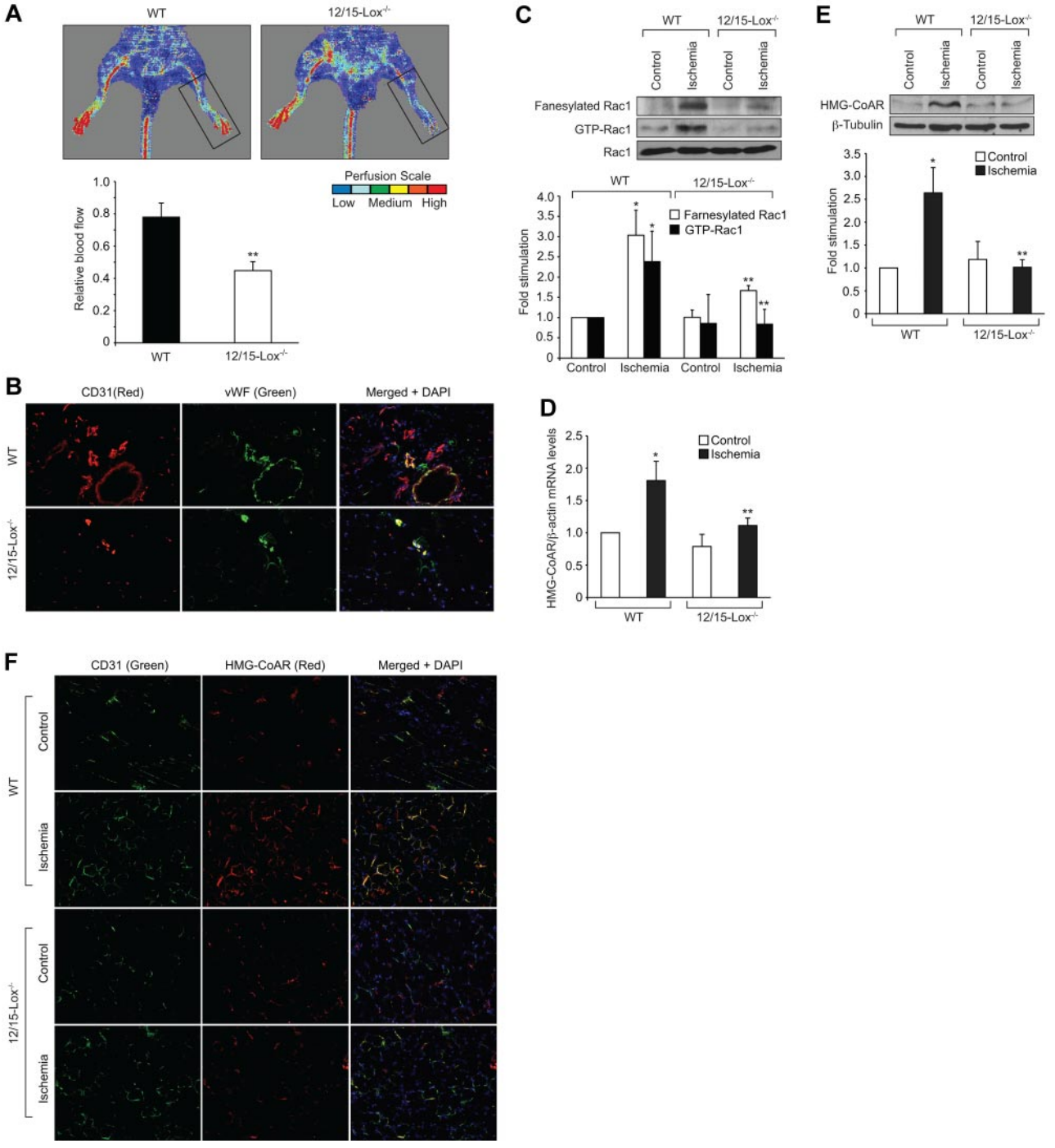

Figure 5. Lack of 12/15-Lox gene impairs blood flow recovery after ischemia. WT and 12/15-Lox$^{-/-}$ mice were subjected to hind-limb ischemia by left femoral artery excision. (A) On day 7 after hind-limb ischemia, blood flow was measured by Laser Doppler Perfusion Imager (LDPI). Perfusion was expressed as ratio of the ischemic to the non-ischemic hind limb. (B) Blood vessels in the ischemic adductor muscles of WT and 12/15-Lox$^{-/-}$ mice were analyzed by double immunofluorescence staining for CD31 (Red) and vWF (Green). (C) Ischemic and non-ischemic adductor muscle tissue extracts from WT and 12/15-Lox$^{-/-}$ mice were prepared and analyzed for Rac1 fanesylation and activation. (D-E) RNA and protein extracts were prepared from ischemic and non-ischemic adductor muscles of WT and 12/15-Lox$^{-/-}$ mice and analyzed for HMG-CoA reductase mRNA (D) and protein levels (E) by QRT-PCR and Western blotting, respectively, as described in Figure 3. (F) Ischemic and non-ischemic adductor muscle sections of WT and 12/15-Lox$^{-/-}$ mice were stained for CD31 (green) and HMG-CoA reductase (red). The bar graphs in panels A, C, D and E represent the mean ± SD values of 3 independent experiments or 6 animals. *$P < .05$ versus WT non-ischemia; **$P < .05$ versus WT ischemia.

of HMG-CoA reductase in 15(S)-HETE–induced angiogenesis can be further strengthened by the observations that exogenous addition of mevalonate rescues 15(S)-HETE–induced farnesylation of Rac1, its membrane translocation and activation from inhibition by simvastatin. As mevalonate also restored 15(S)-HETE–induced migration and tube formation of HDMVECs from inhibition by simvastatin, it is likely that HMG-CoA reductase-dependent Rac1 activation is crucial for the angiogenic effects of 15(S)-HETE in HDMVECs. It may be pointed out that simvastatin while blocking 15(S)-HETE–induced Rac1 farnesylation almost completely, inhibited Rac1 activation by ~ 85%. This small variation between Rac1 farnesylation and its stimulation in response to 15(S)-HETE could be because of basal levels of membrane-associated Rac1 that could be activated by Src-mediated αPix. Because exogenous addition of mevalonate alone was not sufficient to cause

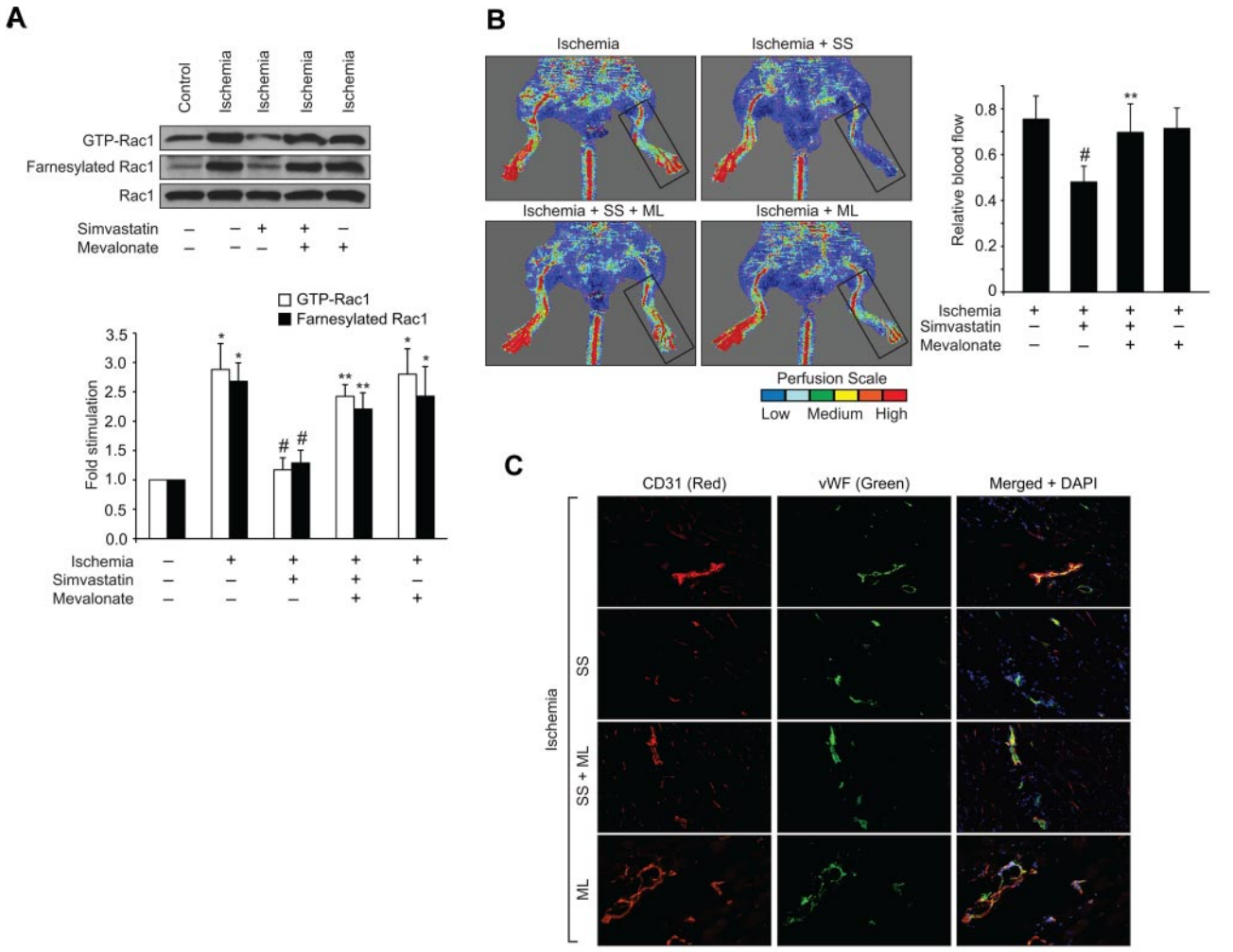

Figure 6. Mevalonate rescues Rac1 farnesylation and activation and blood perfusion from inhibition by simvastatin. (A) Tissue extracts were prepared from ischemic and non-ischemic adductor muscles of WT mice that were administered with or without simvastatin in combination with and without mevalonate and analyzed for Rac1 farnesylation and activation as described in Figure 3. (B) Blood flow was measured by LDPI. (C) Ischemic adductor muscle sections of WT mice that were administered with or without simvastatin in combination with and without mevalonate were stained for CD31 (red) and vWF (green). The bar graphs in panels A and B represent the mean ± SD values of 3 independent experiments or 6 animals. $^{*}P < .05$ versus WT non-ischemia; $^{\#}P < .05$ versus WT ischemia. $^{**}P < .05$ versus WT ischemia + simvastatin.

Rac1 farnesylation and its membrane translocation, it is possible that in addition to its influence on induction of HMG-CoA reductase expression, 15(S)-HETE may also activate other events such as farnesyl transferase (FT) and/or geranylgeranyl transferase (GGT) activities, that are also crucial for farnesylation of Rac1 and its membrane translocation. Although, we have previously demonstrated that Src plays a role in 15(S)-HETE–induced Rac1 activation, the mechanisms by which it mediates this effect was not clear. In this aspect, our present observations reveal that 15(S)-HETE stimulates αPix, a RhoGEF, via Src and it mediates 15(S)-HETE–induced Rac1 activation. Consistent with the role of Rac1 in HDMVEC migration and tube formation, depletion of αPix levels also resulted in the down regulation of these responses.

The in vivo observations reveal that ischemia induces the expression of HMG-CoA reductase and it correlates with the activation of Rac1. In fact, inhibition of HMG-CoA reductase resulted in the suppression of Rac1 activation. It appears that ischemia-induced expression of HMG-CoA reductase is restricted mostly to ECs as shown by double immunofluorescence staining for CD31, a specific marker for EC, and HMG-CoA reductase. Previously, we have reported that hypoxia induces the production of 15(S)-HETE in HRMVECs.[14] Based on these observations, it may be speculated that 15(S)-HETE via inducing the expression of HMG-CoA reductase may mediate hypoxia-induced Rac1 activation and angiogenesis. Indeed, the diminished response of 12/15-Lox$^{-/-}$ mice to ischemia in the induction of HMG-CoA reductase expression and Rac1 farnesylation/activation supports a role for 12/15(S)-HETE in angiogenesis. The involvement of HMG-CoA reductase in 12/15-Lox–induced Rac1 activation and angiogenesis could be demonstrated by the observation that administration of 12/15-Lox$^{-/-}$ mice with mevalonate restores their ability, at least partially, in the activation of Rac1 and formation of new blood vessels in response to ischemia. The finding that 15(S)-HETE–induced Rac1 activation requires HMG-CoA reductase expression and the lack of ability of 12/15-Lox$^{-/-}$ mice to ischemia in the induction of HMG-CoA reductase and Rac1 activation suggest that 12/15(S)-HETE plays an important role in the regulation of this rate-limiting enzyme in the cholesterol biosynthesis. These observations also point out that via its requirement for Rac1 farnesylation, HMG-CoA reductase plays a crucial role in the signaling events that are involved in the modulation of endothelial cell migration and tube formation and thereby angiogenesis. Because the supplementation of mevalonate alone did not restore the capacity of 12/15-Lox$^{-/-}$ mice in the stimulation of Rac1 farnesylation/activation and angiogenesis fully as that of WT mice, it is likely that 12/15(S)-HETE besides

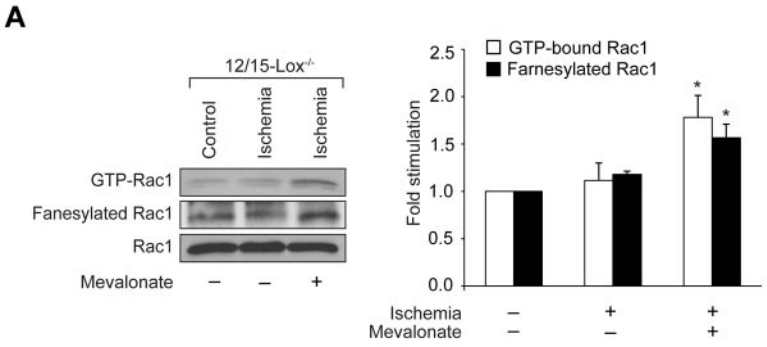

Figure 7. Mevalonate restores the capacity of 12/15-Lox$^{-/-}$ mice to respond to hind-limb ischemia in the induction of Rac1 farnesylation and activation and new blood vessel formation. (A) Tissue extracts were prepared from ischemic and non-ischemic adductor muscles of 12/15-Lox$^{-/-}$ mice that were administered with and without mevalonate and analyzed for Rac1 farnesylation and activation as described in Figure 3. (B) Blood perfusion was measured by LDPI. The bar graphs represent the mean ± SD values of 3 independent experiments or 6 animals. *$P < .05$ versus ischemia.

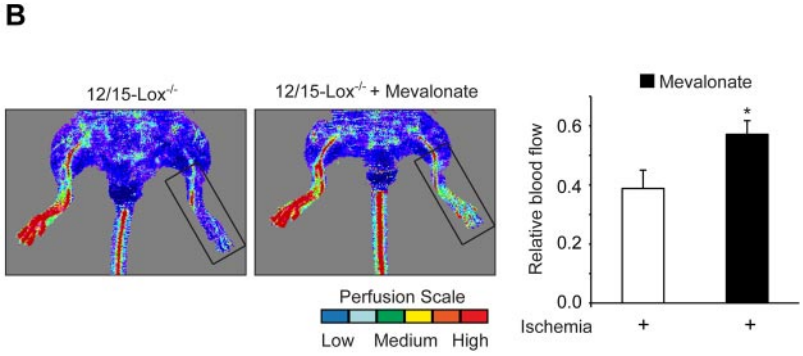

inducing HMG-CoA reductase expression, also modulates other events such as FT/GGT activities in the farnesylation/geranylgeranylation of Rac1 and its heightened activation. Because ischemia induced partial Rac1 farnesylation/activation and angiogenesis in 12/15-Lox$^{-/-}$ mice, it is likely that other eicosanoids or cytokines are produced as a compensatory response to the loss of 12/15-Lox and mediated these partial angiogenic responses. Although, the activation of Src and αPix by ischemia in WT mice suggests a role for these molecules in angiogenesis, it appears that these events are not the major factors for the lack of a response of 12/15-Lox$^{-/-}$

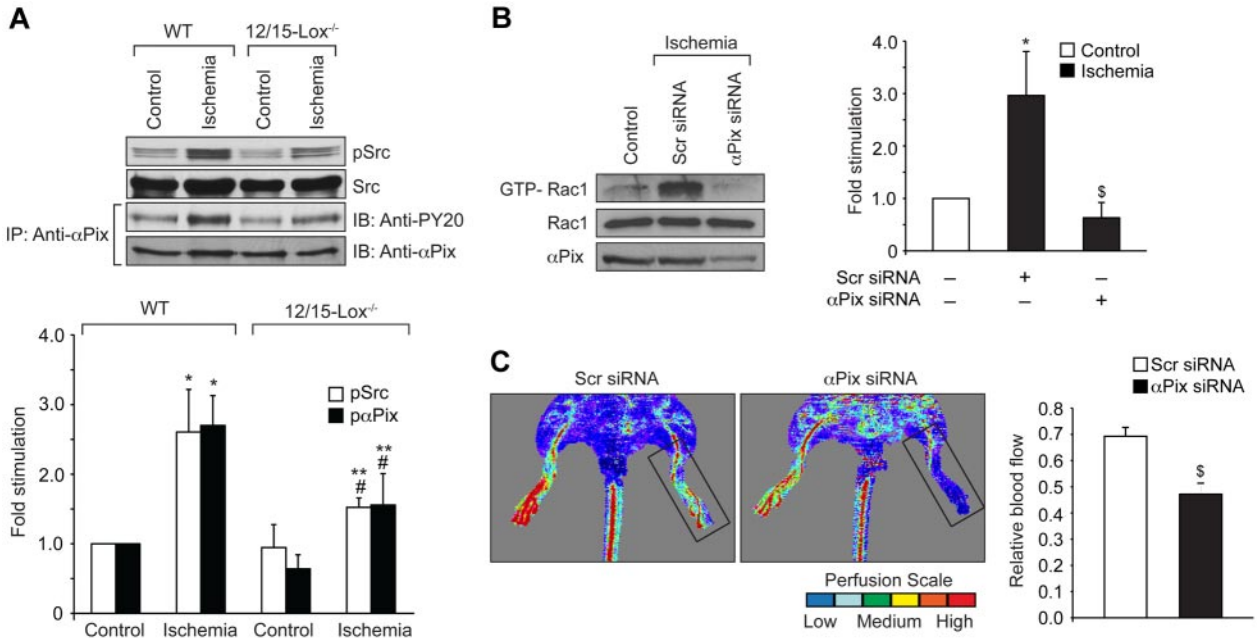

Figure 8. Down-regulation of αPix levels attenuate hind-limb ischemia-induced Rac1 activation and angiogenesis. (A) Tissue extracts were prepared from ischemic and non-ischemic adductor muscles of WT and 12/15-Lox$^{-/-}$ mice and analyzed for Src and αPix activation. To determine Src activation, its tyrosine phosphorylation was measured by Western blotting using its phospho-specific antibodies. Activation of αPix was measured as described in Figure 4A. (B) Tissue extracts were prepared from ischemic and non-ischemic adductor muscles of WT mice that received scrambled or αPix siRNA and analyzed for Rac1 activation by pull-down assay and αPix levels by Western blotting. (C) Blood perfusion was measured by LDPI in WT mice that received scrambled or αPix siRNA in response to ischemia. The bar graph represents the mean ± SD values of 3 independent experiments or 6 animals. *$P < .05$ versus WT non-ischemia; #$P < .05$ versus 12/15-Lox$^{-/-}$ non-ischemia; **$P < .05$ versus WT ischemia; \$$P < .05$ versus WT ischemia + scr siRNA.

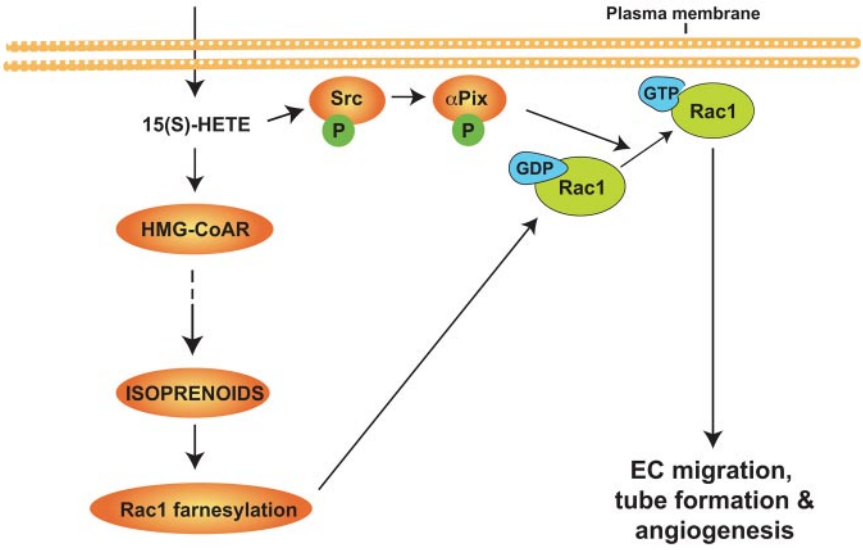

Figure 9. Schematic diagram showing the role of HMG-CoA reductase in 12/15-Lox–12/15(S)-HETE–induced angiogenesis.

mice to hind-limb ischemia-induced angiogenesis as they are also activated in these mice, although to a lesser extent. It was reported that 12/5-Lox knockout prevents the development of atherosclerosis in ApoE$^{-/-}$ mice.[38,39] Many studies have reported that intraplaque angiogenesis plays a role in plaque rupture and therefore causes thrombus formation.[40,41] Previous studies have also reported that atherosclerotic arteries convert arachidonic acid preferentially to 15-HETE.[42,43] Because 15-HETE is produced in atherosclerotic arteries and 12/15-Lox-12/15(S)-HETE axis induces angiogenesis, it is possible that these lipid molecules may play a role in the development of intraplaque angiogenesis. Similarly, many reports have indicated that 12/15(S)-HETE promotes cancer development particularly prostate cancer.[44-46] Therefore, one mechanism by which these lipid molecules could influence tumor growth is via their involvement in the stimulation of angiogenesis. In this aspect, the present findings that 12/15-Lox$^{-/-}$ mice lack the capacity to ischemia-induced HMG-CoA reductase expression and Rac1 farnesylation, provide a compelling evidence for the role of this AA metabolizing enzyme in tumor growth and vascular diseases. In addition, it is important to point out that many reports showed that statins, which were shown to have beneficial effects in the prevention of both cancer and vascular diseases, inhibit angiogenesis,[47-50] although some reports demonstrated the opposite effects.[48] The induction of angiogenesis by statins at lower doses as observed by some studies could be mediated via mechanisms that are independent of their effects on HMG-CoA reductase.

In brief, as shown the Figure 9, the present study provides the first evidence for the role of HMG-CoA reductase in 12/15-LOX–12/15(S)-HETE–induced angiogenesis. The present findings may also suggest that approaches targeting inhibition of 12/15-LOX may be more effective in the treatment of cancer and vascular diseases.

Acknowledgments

This work was supported by grants HL016465 and HL074860 from the National Heart, Lung, and Blood Institute/National Institutes of Health to G.N.R.

Authorship

Contribution: N.K.S. performed cell migration assay, hind-limb ischemia, immunofluorescence analysis, pull-down assays, and tube formation assay; V.K.S. performed pull-down assays, cell migration, tube formation, and immunofluorescence analysis; and G.N.R. designed the experiments, interpreted data, and wrote the paper.

Conflict-of-interest disclosure: The authors declare no competing financial interests.

Correspondence: Gadiparthi N. Rao, PhD, Department of Physiology, University of Tennessee Health Science Center, 894 Union Ave, Memphis, TN 38163; e-mail: rgadipar@uthsc.edu.

References

1. Folkman J. Angiogenesis in cancer, vascular, rheumatoid and other disease. *Nat Med.* 1995; 1(1):27-31.
2. Freedman SB, Isner JM. Therapeutic angiogenesis for ischemic cardiovascular disease. *J Mol Cell Cardiol.* 2001;33(3):379-393.
3. Ferrara N, Alitalo K. Clinical applications of angiogenic growth factors and their inhibitors. *Nat Med.* 1999;5(12):1359-1364.
4. Carmeliet P, Ng YS, Nuyens D, et al. Impaired myocardial angiogenesis and ischemic cardiomyopathy in mice lacking the vascular endothelial growth factor isoforms VEGF164 and VEGF188. *Nat Med.* 1999;5(5):495-502.
5. Fahmy RG, Dass CR, Sun LQ, Chesterman CN, Khachigian LM. Transcription factor Egr-1 supports FGF-dependent angiogenesis during neovascularization and tumor growth. *Nat Med.* 2003;9(8):1026-1032.
6. Sparmann A, Bar-Sagi D. Ras-induced interleukin-8 expression plays a critical role in tumor growth and angiogenesis. *Cancer Cell.* 2004;6(5):447-458.
7. Hong KH, Ryu J, Han KH. Monocyte chemoattractant protein-1-induced angiogenesis is mediated by vascular endothelial growth factor-A. *Blood.* 2005;105(4):1405-1407.
8. Skoura A, Sanchez T, Claffey K, Mandala SM, Proia RL, Hla T. Essential role of sphingosine 1-phosphate receptor 2 in pathological angiogenesis of the mouse retina. *J Clin Invest.* 2007; 117(9):2506-2516.
9. Murakami M, Simons M. Fibroblast growth factor regulation of neovascularization. *Curr Opin Hematol.* 2008;15(3):215-220.
10. Mezentsev A, Seta F, Dunn MW, Ono N, Falck JR, Laniado-Schwartzman M. Eicosanoid regulation of vascular endothelial growth factor expression and angiogenesis in microvessel endothelial cells. *J Biol Chem.* 2002;277(21):18670-18676.
11. Zhang B, Cao H, Rao GN. 15(S)-hydroxyeicosatetraenoic acid induces angiogenesis via activation of PI3K-Akt-mTOR-S6K1 signaling. *Cancer Res.* 2005;65(16):7283-7291.
12. Zhang B, Cao H, Rao GN. Fibroblast growth factor-2 is a downstream mediator of phosphatidylinositol 3-kinase-Akt signaling in 14,15-epoxyeicosatrienoic acid-induced angiogenesis. *J Biol Chem.* 2006;281(2):905-914.

13. Srivastava K, Kundumani-Sridharan V, Zhang B, Bajpai AK, Rao GN. 15(S)-hydroxyeicosatetraenoic acid-induced angiogenesis requires STAT3-dependent expression of VEGF. *Cancer Res.* 2007;67(9):4328-4336.
14. Bajpai AK, Blaskova E, Pakala SB, et al. 15(S)-HETE production in human retinal microvascular endothelial cells by hypoxia: Novel role for MEK1 in 15(S)-HETE induced angiogenesis. *Invest Ophthalmol Vis Sci.* 2007;48(11):4930-4938.
15. Cheranov SY, Karpurapu M, Wang D, Zhang B, Venema RC, Rao GN. An essential role for SRC-activated STAT-3 in 14,15-EET-induced VEGF expression and angiogenesis. *Blood.* 2008; 111(12):5581-5591.
16. Finetti F, Donnini S, Giachetti A, Morbidelli L, Ziche M. Prostaglandin E(2) primes the angiogenic switch via a synergic interaction with the fibroblast growth factor-2 pathway. *Circ Res.* 2009;105(7):657-666.
17. Cheranov SY, Wang D, Kundumani-Sridharan V, et al. The 15(S)-hydroxyeicosatetraenoic acid-induced angiogenesis requires Janus kinase 2-signal transducer and activator of transcription-5B-dependent expression of interleukin-8. *Blood.* 2009;113(23):6023-6033.
18. Connor KM, SanGiovanni JP, Lofqvist C, et al. Increased dietary intake of omega-3-polyunsaturated fatty acids reduces pathological retinal angiogenesis. *Nat Med.* 2007;13(7):868-873.
19. Szymczak M, Murray M, Petrovic N. Modulation of angiogenesis by omega-3 polyunsaturated fatty acids is mediated by cyclooxygenases. *Blood.* 2008;111(7):3514-3521.
20. Herbert SP, Odell AF, Ponnambalam S, Walker JH. Activation of cytosolic phospholipase A2-{alpha} as a novel mechanism regulating endothelial cell cycle progression and angiogenesis. *J Biol Chem.* 2009;284(9):5784-5796.
21. Matsumoto H, Ma WG, Daikoku T, et al. Cyclooxygenase-2 differentially directs uterine angiogenesis during implantation in mice. *J Biol Chem.* 2002;277(32):29260-29267.
22. Cha YI, Solnica-Krezel L, DuBois RN. Fishing for prostanoids: deciphering the developmental functions of cyclooxygenase-derived prostaglandins. *Dev Biol.* 2006;289(2):263-272.
23. Zhao T, Wang D, Cheranov SY, et al. A novel role for activating transcription factor-2 in 15(S)-hydroxyeicosatetraenoic acid-induced angiogenesis. *J Lipid Res.* 2009;50(3):521-533.
24. Kundumani-Sridharan V, Niu J, Wang D, et al. 15(S)-hydroxyeicosatetraenoic acid-induced angiogenesis requires Src-mediated Egr-1-dependent rapid induction of FGF-2 expression. *Blood.* 2010;115(10):2105-2116.
25. Singh NK, Quyen DV, Kundumani-Sridharan V, Brooks PC, Rao GN. AP-1 (Fra-1/c-Jun)-mediated induction of expression of matrix metalloproteinase-2 is required for 15(S)-hydroxyeicosatetraenoic acid-induced angiogenesis. *J Biol Chem.* 2010;285(22): 16830-16843.
26. Schlessinger J. New roles for Src kinases in control of cell survival and angiogenesis. *Cell.* 2000; 100(3):293-296.
27. Eliceiri BP, Paul R, Schwartzberg PL, Hood JD, Leng J, Cheresh DA. Selective requirement for Src kinases during VEGF-induced angiogenesis and vascular permeability. *Mol Cell.* 1999;4(6): 915-924.
28. Etienne-Manneville S, Hall A. Rho GTPases in cell biology. *Nature.* 2002;420(6916):629-635.
29. Raftopoulou M, Hall A. Cell migration: Rho GTPases lead the way. *Dev Biol.* 2004;265(1):23-32.
30. Liu WF, Nelson CM, Pirone DM, Chen CS. E-cadherin engagement stimulates proliferation via Rac1. *J Cell Biol.* 2006;173(3):431-441.
31. Liu Z, Zhang C, Dronadula N, Li Q, Rao GN. Blockade of nuclear factor of activated T cells activation signaling suppresses balloon injury-induced neointima formation in a rat carotid artery model. *J Biol Chem.* 2005;280(15):14700-14708.
32. Park HJ, Galper JB. 3-Hydroxy-3-methylglutaryl CoA reductase inhibitors up-regulate transforming growth factor-beta signaling in cultured heart cells via inhibition of geranylgeranylation of RhoA GTPase. *Proc Natl Acad Sci U S A.* 1999;96(20): 11525-11530.
33. Thorpe JL, Doitsidou M, Ho SY, Raz E, Farber SA. Germ cell migration in zebrafish is dependent on HMGCoA reductase activity and prenylation. *Dev Cell.* 2004;6(2):295-302.
34. Rossman KL, Der CJ, Sondek J. GEF means go: turning on RHO GTPases with guanine nucleotide-exchange factors. *Nat Rev Mol Cell Biol.* 2005;6(2): 167-180.
35. Baird D, Feng Q, Cerione RA. The Cool-2/alpha-Pix protein mediates a Cdc42-Rac signaling cascade. *Curr Biol.* 2005;15(1):1-10.
36. Willey JZ, Elkind MS. 3-Hydroxy-3-methylglutaryl-coenzyme A reductase inhibitors in the treatment of central nervous system diseases. *Arch Neurol.* 2010;67(9):1062-1067.
37. Dai Y, Khanna P, Chen S, Pei XY, Dent P, Grant S. Statins synergistically potentiate 7-hydroxystaurosporine (UCN-01) lethality in human leukemia and myeloma cells by disrupting Ras farnesylation and activation. *Blood.* 2007;109(10):4415-4423.
38. Cyrus T, Witztum JL, Rader DJ, et al. Disruption of the 12/15-lipoxygenase gene diminishes atherosclerosis in apo E-deficient mice. *J Clin Invest.* 1999;103(11):1597-1604.
39. Poeckel D, Zemski Berry KA, Murphy RC, Funk CD. Dual 12/15- and 5-lipoxygenase deficiency in macrophages alters arachidonic acid metabolism and attenuates peritonitis and atherosclerosis in ApoE knock-out mice. *J Biol Chem.* 2009;284(31):21077-21089.
40. Leroyer AS, Rautou PE, Silvestre JS, et al. CD40 ligand+ microparticles from human atherosclerotic plaques stimulate endothelial proliferation and angiogenesis a potential mechanism for intraplaque neovascularization. *J Am Coll Cardiol.* 2008;52(16):1302-1311.
41. Koutouzis M, Nomikos A, Nikolidakis S, et al. Statin treated patients have reduced intraplaque angiogenesis in carotid endarterectomy specimens. *Atherosclerosis.* 2007;192(2):457-463.
42. Henriksson P, Hamberg M, Diczfalusy U. Formation of 15-HETE as a major hydroxyeicosatetraenoic acid in the atherosclerotic vessel wall. *Biochim Biophys Acta.* 1985;834(2):272-274.
43. Simon TC, Makheja AN, Bailey JM. Formation of 15-hydroxyeicosatetraenoic acid (15-HETE) as the predominant eicosanoid in aortas from Watanabe Heritable Hyperlipidemic and cholesterol-fed rabbits. *Atherosclerosis.* 1989;75(1):31-38.
44. Shappell SB, Olson SJ, Hannah SE, et al. Elevated expression of 12/15-lipoxygenase and cyclooxygenase-2 in a transgenic mouse model of prostate carcinoma. *Cancer Res.* 2003;63(9): 2256-2267.
45. Kelavkar UP, Glasgow W, Olson SJ, Foster BA, Shappell SB. Overexpression of 12/15-lipoxygenase, an ortholog of human 15-lipoxygenase-1, in the prostate tumors of TRAMP mice. *Neoplasia.* 2004;6(6):821-830.
46. Gonzalez AL, Roberts RL, Massion PP, Olson SJ, Shyr Y, Shappell SB. 15-Lipoxygenase-2 expression in benign and neoplastic lung: an immunohistochemical study and correlation with tumor grade and proliferation. *Hum Pathol.* 2004;35(7): 840-849.
47. Park HJ, Kong D, Iruela-Arispe L, Begley U, Tang D, Galper JB. 3-Hydroxy-3-methylglutaryl coenzyme A reductase inhibitors interfere with angiogenesis by inhibiting the geranylgeranylation of RhoA. *Circ Res.* 2002;91(2):143-150.
48. Urbich C, Dernbach E, Zeiher AM, Dimmeler S. Double-edged role of statins in angiogenesis signaling. *Circ Res.* 2002;90(6):737-744.
49. Demierre MF, Higgins PD, Gruber SB, Hawk E, Lippman SM. Statins and cancer prevention. *Nat Rev Cancer.* 2005;5(12):930-942.
50. Zhu BQ, Heeschen C, Sievers RE, et al. Second hand smoke stimulates tumor angiogenesis and growth. *Cancer Cell.* 2003;4(3):191-196.